Research paper

Fundamental study on rock fracture mechanism induced by blasting in small-scale blasting tests

Yoshiaki Takahashi*†, Tei Saburi**, Takashi Sasaoka*, Sugeng Wahyudi*, Shiro Kubota**, Hideki Shimada*, and Yuji Ogata**

*Kyushu University, 744 Motooka, Nishi, Fukuoka-shi, Fukuoka, 819−0395 JAPAN
Phone: +81−090−7537−5786
†Corresponding author: takahashi13r@mine.kyushu-u.ac.jp

**National Institute of Advanced Industrial Science and Technology, 16−1 Onogawa, Tsukuba-shi, Ibaraki, 305−8569 JAPAN

Received: January 11, 2018 Accepted: August 10, 2018

Abstract

Rock blasting is one of the most commonly used technique in open-pit mining in terms of economic and efficiency. This technique, however, can cause serious accidents or environmental impacts such as flyrock, ground vibration or noise. In order to control such negative impacts, rock fracture mechanism induced by blasting should be theoretically considered. For this reason, small-scale blasting test with mortar block was performed in this research. Strain profile of the surface on the mortar block was analyzed by means of digital image correlation (DIC) method based on a series of photographs taken by two high speed cameras. According to the results, the value of both lateral and longitudinal strain gradually increased from approximately 50 μs after the detonation which is the arrival time of S-wave from the blasting sources; therefore, it can be said dynamic strain can be assessed by DIC. As a next step, strain rate was calculated for further discussions. The results show that strain rate strongly influence on crack generation and crack growth.

Keywords: blasting, surface mining, scaled experiment, digital image correlation

1. Introduction

Rock blasting is one of the most essential process in open-pit mining excavation in terms of economic and efficiency[1]. The application of this blasting technique, however, has been strictly regulated by law because it may cause serious accidents or environmental impacts such as ground vibration, flyrock or noise[2]. Rock fracture mechanism induced by blasting should be theoretically understood in order to control such negative impacts. Although a number of field experiment results have been reported, it is difficult to discuss the mechanism since rock mass conditions are different from each mine and blast face.

For this reason, we have conducted small-scale blasting experiment with mortar block. In order to discuss rock fracture mechanism, strain of free face have evaluated by strain gauge. Nevertheless, accurate measurement could not been performed because of electrical noise on strain signal induced by detonation of detonator[3]. In addition, although wave interference generally influence on crack generation, a gauge can only evaluate point information even if a number of gauges are applied to the measurement.

Therefore, in order to solve above problems, the application of digital image correlation (DIC) method is discussed in this study. Two-dimensional strain distribution on surface of free face during blasting was visualized and quantitatively evaluated by applying DIC method. Then, crack generation and growth are discussed based on the DIC results.

2. Experiment

2.1 Outline of small-scale blasting experiment

Small-scale blasting test was performed with mortar blocks as shown in Figure 1. The block was 100 cm wide, 50 cm deep and 60 cm height. Two blasting holes with 13 mm in diameter and 200 mm in length were arranged in one row. Both burden and hole spacing were 100 mm. As

Table 1 Mechanical property of mortar block.

Dimension	100 × 60 × 40[cm]		
Composition	mixing ratio	cement:water:sand	1770:919:5311
	sand material	surface-dry density	2.62 g cm^{-3}
		absolute-dry density	2.56 g cm^{-3}
		rate of water absorption	2.18%
		the fineness modulus	2.83
Nominal strength	21 N mm^{-2}		
Mean strength	23 N mm^{-2}		
P wave velocity	3,557 m s^{-1}		
S wave velocity	2,102 m s^{-1}		

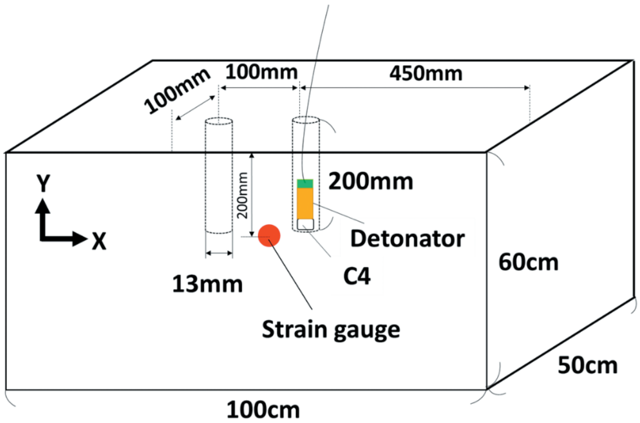

Figure 1 Outline of mortar block and blasting designs.

explosives, one exploding bridgewire detonator (EBW) with 1.3 g composition C4 was inserted into the bottom of each blasting hole. In this test, EBW detonator was adopted since time accuracy of detonation of detonator may be over shooting time by high-speed cameras. Each of two ignition control units charged a firing module up to firing voltage of 4,000 V for arming and each of the firing modules fired by EBW detonator by an external trigger from digital delay generator. Moreover, for the purpose of comparison, biaxial strain gauge was attached on the surface at the center of bottom of two blasting hole as shown in Figure 1. Mechanical properties of the mortar block is listed in Table 1. In this study, strain in x and y direction shown in Figure 1 are defined as ε_{xx} and ε_{yy}, respectively.

2.2 Digital image correlation (DIC)

DIC method can analyze displacement/strain of shooting area on a basis of digital images taken by camera (s)[4]. In this analysis method, deformation and direction of the random pattern (speckle) drawn on evaluation area are visually traced by a correlation algorithm with a grey scale $G(x, y)$ of a pixel position (x, y) in images[5),6)]. In other words, this method is non-contact and optical measurement system; therefore it is not affected by electrical noise and two or three dimensional analysis can be performed. Additionally, the method has wide dynamic range of strain and high sensitivity (1/100,000 of field of view). This method have started to apply to the field of

Table 2 Shooting conditions of high-speed cameras.

	Left : SHIMADZU HPV-X	Right : SHIMADZU HPV-1
Recording speed	500,000fps	
Exposure	1/1,000,000 [s]	1/1,000,000 [s]
Resolution	400 × 250	312 × 260
Lens	Tokina AT-X 840D 120 mm F3.5	220 mm F3.5

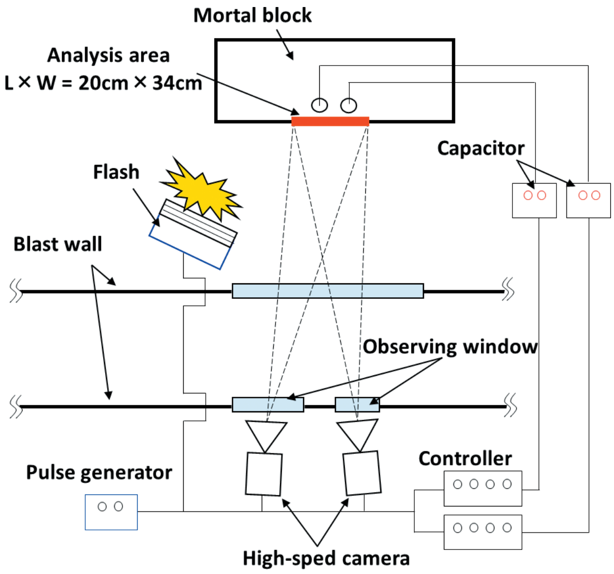

Figure 2 Arrangement of equipment and sample.

rock mechanics[7)].

For DIC analysis, random patterns (speckle) were drawn on the front surface of the mortar block. Series of photographs during blasting were taken by two high-speed cameras (SHIMADZU, HPV-1 and HPV-X) every 2 μs. It means the sampling rate of the analysis is 2 μs. Based on the photographs, DIC analysis was performed by the software, VIC-3D (Correlated Solutions). The other shooting conditions of high-speed cameras are listed in Table 2. In addition, Figure 2 is an illustration of the arrangement of equipment. High-speed cameras and flash light were also triggered by digital delay signal. Before the experiment, the DIC system was calibrated with a planar calibration method[8)].

3. Results and discussions

3.1 Applicability of DIC method

The result of strain profile recorded by strain gauge and that of point a (analysis point on strain gauge) analyzed by DIC are shown in Figure 3 (a) and (b), respectively. According to Figure 3 (a), both ε_{xx} and ε_{yy} immediately change after the detonation of detonator. In addition, recorded both strain values are too large for brittle material. This is because electrical noise is induced by the firing pulse for EBW detonator. On the other hand, as shown in Figure 3 (b), both lateral and longitudinal strains gradually increase from approximately 50 μs after the detonation. This time is good accordance with arrival time of elastic wave (S wave) from the blasting holes to analysis point and the value of calculated strain is reasonable according to past researches[9), 10)]. On the other hand, the strain induced by P wave was could not be detected due to the accuracy of this analysis in this study. Furthermore, as shown in Figure 4, crack occurrence can be recognized where tensile strain is higher than 7×10^{-9} by DIC. On a basis of these results, it can be said that high speed strain of brittle material induced by blasting is assessed by applying DIC method.

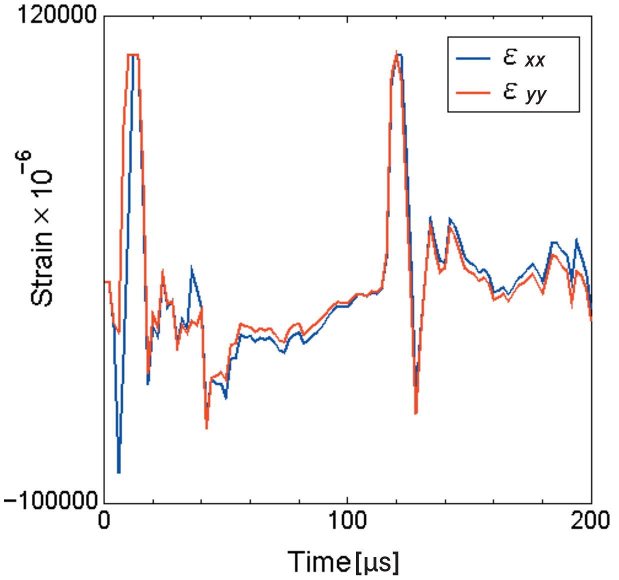

(a)

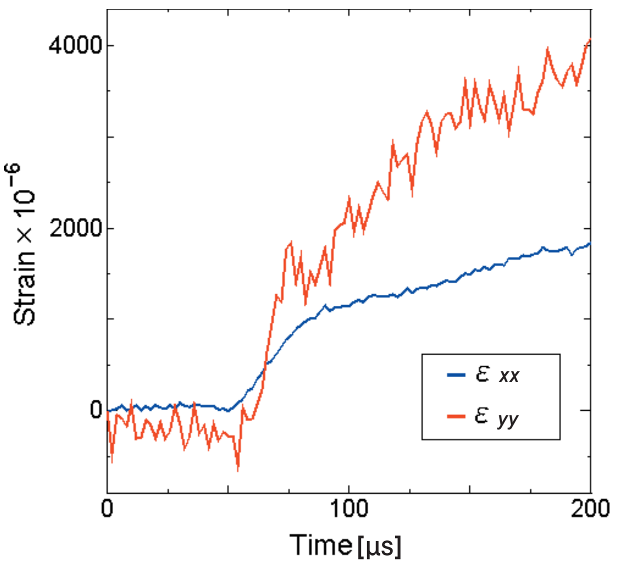

(b)

Figure 3 Strain histories on the point of interest: (a) measured by strain gauge, (b) analyzed by DIC.

3.2 Rock fracture mechanism on free face

Based on the strain distribution analyzed by DIC, fracture mechanism on free face induced by blasting is discussed in this section. Two analysis lines are set as shown in Figure 5: line AB which is through the crack and line CD which is not through the crack. In addition, two analysis points are also set on line AB and line CD, respectively; point b is the starting point of crack and point c is the point above point b. By considering the direction of the propagated crack during analysis time, the ε_{yy} histories of both lines every 20 μs are shown in Figure 6 (a) and (b), respectively. As shown in Figure 6 (a), large strain was recorded around the area above two blasting holes. On the other hand, the ε_{yy} above the center between two blasting hole was larger than other area on line CD as shown in Figure 6 (b). This is because stress wave interference lead the change of stress and strain distribution.

Although strain distribution is different, there is not huge difference of the value of recorded strain between two lines. In other words, by only considering the value of strain, crack could occur on line CD, especially around the center between two blasting hole like point c. Moreover, in this experiment, crack appeared from point b on line AB

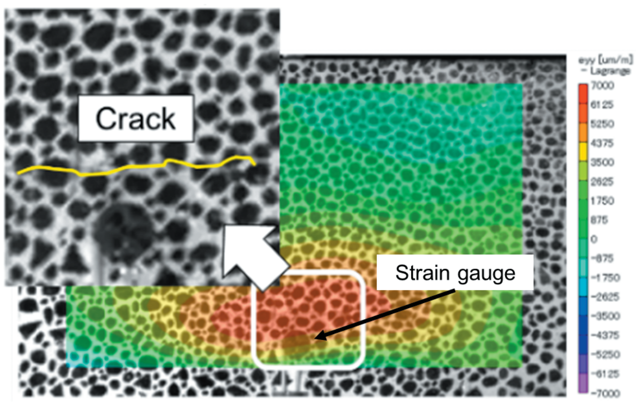

Figure 4 Recognition of the crack occurrence in high tensile strain area at 200μs after blasting.

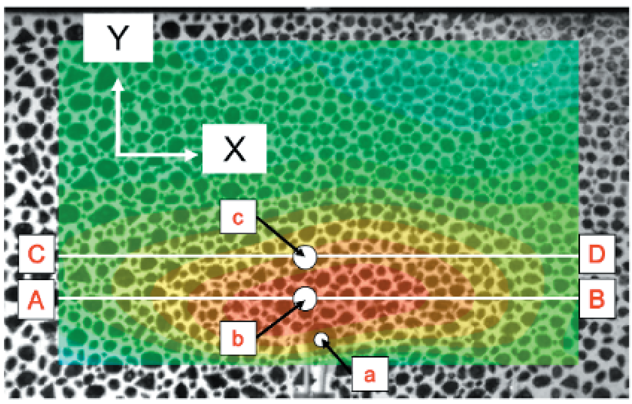

Figure 5 Analysis lines and points.

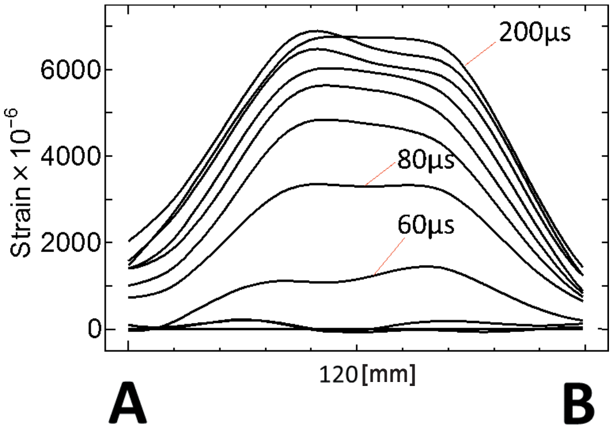

(a)

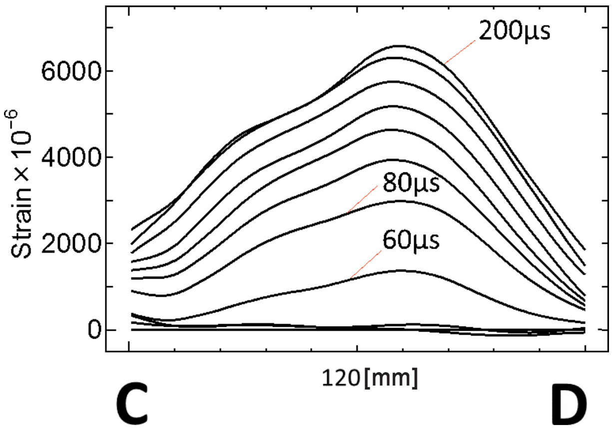

(b)

Figure 6 ε_{yy} profile. (a) along with line AB and (b) along with line CD.

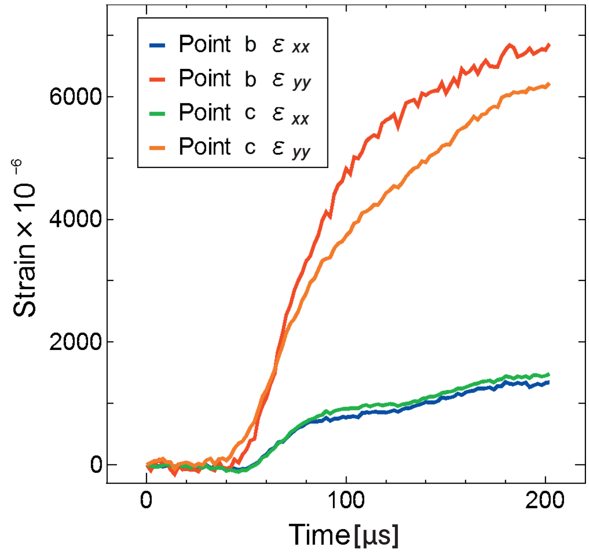

(a)

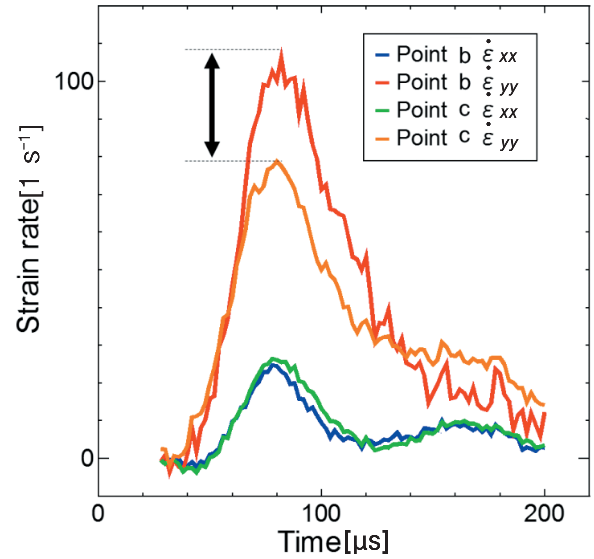

(b)

Figure 7 (a) Strain history at points b and c. (b) Strain rate history at points b and c (15 moving average).

at approximately 70 μs after the detonation. This result indicated that there is other factor which influence on crack generation except for strain. By comparing ε_{yy} histories of both lines, there is clear difference of the amount of change of strain between 60 μs and 80 μs. In other words, strain rate can effect on the crack generation. For this, strain history and strain rate history (15 moving average) of point b on line AB and point c on line CD are compared as shown in Figure 7 (a) and (b), respectively. As shown in these figures, there are clear difference of strain rate of ε_{yy} ($\dot{\varepsilon}_{yy}$) although large strain difference cannot be seen between point b and c. It can be said that not only strain but also strain rate strongly influence on crack occurrence.

Hence, as a next step, 10 points are extracted from line AB and $\dot{\varepsilon}_{yy}$ of these points are analyzed and compared as shown in Figure 8 in order to discuss crack growth. As can be seen in Figure 8, all strain rates at all points reach their peak at the same time and $\dot{\varepsilon}_{yy}$ of points on crack record over a certain value. In other words, crack occurred and propagated to the area where strain rate is over a certain value at a certain timing. In this experiment, crack can be recognized at the points where $\dot{\varepsilon}_{yy}$ is over approximately 100 s^{-1}.

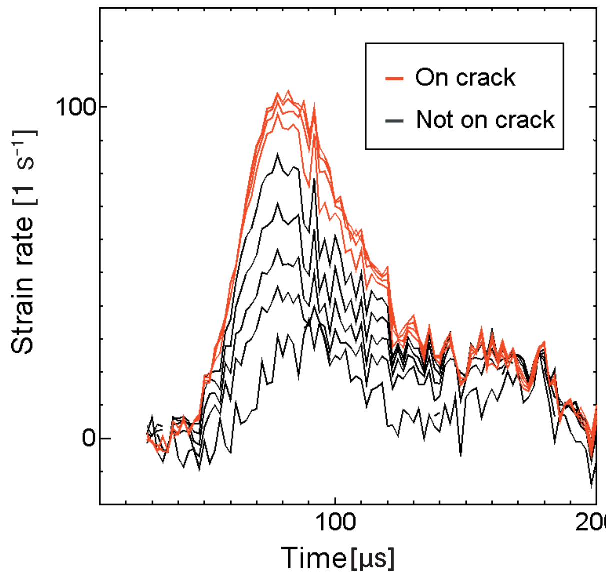

Figure 8 Strain rate history of ε_{yy} at 10 points on line AB (15 moving average).

4. Conclusions

Applicability of DIC method to scaled blasting experiment and crack generation and propagation on a basis of DIC analysis are discussed in this paper. Based on the results, it can be said DIC can be successfully applied to analysis of high-speed fracture phenomena of brittle material. Two-dimensional strain information can be quantitatively visualized and evaluated. Moreover, in terms of rock fracture mechanism, it is made clear that crack generation is strongly related to not only strain but also strain rate, and crack propagate to the area where strain rate is over a certain value at a certain timing. In this study, crack extend to the area where strain rate is over approximately 100 s^{-1}.

References

1) M. Monjezi, A. Bahrami, and A. Y. Varjani, Int. J. Rock Mech. Min. Sci., 47, 476–480 (2010).
2) K. Matsui and H. Shimada, J. Limestone, 330, 57–61 (2004). (in Japanese).
3) Y. Takahashi, T. Saburi, T. Sasaoka, S. Wahyudi, S. Kubota, H. Shimada, and Y. Ogata, Proc. MMIJ Spring Meeting (2016). (in Japanese).
4) T. P. Chu, W. F. Ranson, and M. Sutton, Experimental Mech., 25, 232–244 (1985).
5) M. A. Sutton, J. J. Orteu, and H. W. Schreier, “Image Correlation for Shape, Motion and Deformation Measurement”, Springer Science and Business Media (2009).
6) T. Saburi, Y. Takahashi, S. Kubota, and Y. Ogata, M.S.F., 910, 161–166 (2018).
7) H. Munoz, A. Taheri, and E. K. Chanda, Rock Mec. Rock Eng., 49, 2541–2544 (2016).
8) C. H. Hwang, W. C. Wang, and Y. H. Chen, Proc. 37th NCTAM 2013 & The 1st ICM (2013).
9) M. Beppu, K. Miwa, and J. Takahashi, J. Japan Society of Civil Eng., 68, 398–412 (2012).
10) M. Beppu, K. Miwa, T. Ono, and M. Siomi, J. Japan Society of Civil Eng., 63, 178–191 (2007).